

Analysing the isotopic life history of the alpine ungulates *Capra ibex* and *Rupicapra rupicapra rupicapra* through their horns

Inês C. R. Barbosa¹, Maximiliane Kley¹, Rudi Schäufele¹, Karl Auerswald¹, Wolf Schröder², Flurin Filli³, Stefan Hertwig⁴ and Hans Schnyder^{1*}

¹Lehrstuhl für Grünlandlehre, Technische Universität München, Germany

²Fachgebiet Wildbiologie, Technische Universität München, Germany

³Parc Naziunal Svizzer, Schloss Planta-Wildenberg, Zerne, Switzerland

⁴Naturhistorisches Museum der Burgergemeinde, Bern, Switzerland

Received 12 March 2009; Revised 5 June 2009; Accepted 11 June 2009

The horn of ungulate grazers offers a valuable isotopic record of their diet and environment. However, there have been no reports of the spatio-temporal variation of the isotopic composition of horns. We investigated patterns of carbon ($\delta^{13}\text{C}$) and nitrogen ($\delta^{15}\text{N}$) isotopic composition along and perpendicular to the horn axis in *Capra ibex* and *Rupicapra rupicapra rupicapra* to assess the effects of animal age, within-year (seasonal) and inter-annual variation, natural contamination and sampling position on horn isotope composition. Horns of male *C. ibex* ($n = 23$) and *R. r. rupicapra* ($n = 1$) were sampled longitudinally on the front (only *R. r. rupicapra*) and back side and on the surface and sub-surface. The sides of the *R. r. rupicapra* horn did not differ in $\delta^{13}\text{C}$. In both species, the horn surface had a 0.15‰ lower $\delta^{13}\text{C}$ and a higher carbon-to-nitrogen (C/N) ratio than the sub-surface. Washing the horn with water and organic solvents removed material that caused these differences. With age, the $\delta^{15}\text{N}$ of *C. ibex* horns increased (+0.1‰ year⁻¹), C/N ratio increased, and ^{13}C discrimination relative to atmospheric CO_2 ($^{13}\Delta$) increased slightly (+0.03‰ year⁻¹). Geostatistical analysis of one *C. ibex* horn revealed systematic patterns of inter-annual and seasonal ^{13}C changes, but ^{15}N changed only seasonally. The work demonstrates that isotopic signals in horns are influenced by natural contamination ($\delta^{13}\text{C}$), age effects ($^{13}\Delta$ and $\delta^{15}\text{N}$), and seasonal ($\delta^{13}\text{C}$ and $\delta^{15}\text{N}$) and inter-annual variation ($\delta^{13}\text{C}$). The methods presented allow us to distinguish between these effects and thus allow the use of horns as isotopic archives of the ecology of these species and their habitat. Copyright © 2009 John Wiley & Sons, Ltd.

Based on the principle stated by DeNiro and Epstein¹ ‘‘You are what you eat, isotopically’’ for decades many studies in animal ecology have applied isotope techniques to characterise and quantify diet inputs, measure trophic interactions, trace large-scale movements and assess general nutritional condition.^{2–8} The wide application of these techniques in animal ecology is based on the fact that several biogeochemical processes produce systematic variations in the natural isotope abundance that is passed from primary producers onto consumer food webs. Animal tissues become labelled with the isotopic composition of their diet. The extent of this labelling depends on the isotope fractionation characteristic of the tissues and on their metabolic turnover rates.⁹

Most isotope studies designed to track migrants or describe temporal variation of diet composition have used metabolically inert tissues for which growth periods and rates are well defined.^{7,10} Metabolically inert tissues are the ones

which are progressively laid down and remain unchanged, so that the stable isotope ratios are locked during their growth. These tissues include hair, claws, feathers, baleen and teeth.^{6,11} Isotopic chronologies can be reconstructed from the spatial variation of isotope composition along the growth axis of the horn and knowledge of the timing and rate of tissue growth.^{6,11–14}

These works allowed new insights in animal ecology, such as tracing whale migration patterns,¹⁵ diet and foraging behaviour of elephants,¹⁰ and altitudinal distribution and movement of birds.¹⁶ Recent studies have also shown the potential of hair as archives of biogeochemical processes in grassland: there is a strong correlation between the ^{13}C signature of grazer hair and that of pasture vegetation at different levels of plant-available soil water.¹⁷ In addition, altitudinal variation in ^{13}C (or ^{15}N) of grazer hair corresponds closely with that of pasture vegetation along the same altitude gradients.¹⁸

The horns of ungulates, like hair, are a hard metabolically inert α -keratinous tissue. Hard keratins are very stable proteins, insoluble in conventional protein solvents,¹⁹ and essentially resistant against proteolytic enzymes and *post*

*Correspondence to: H. Schnyder, Lehrstuhl für Grünlandlehre, Technische Universität München, Germany.
E-mail: schnyder@wzw.tum.de

mortem degradation.²⁰ For this reason, keratinous tissues constitute important historical records of species ecology and ecosystems properties. Horn fibre formation follows the general sequence of events of keratinous tissues: cells deriving from a stem cell population undergo differentiation, keratinisation and cornification, with some final structural and anatomical differences.¹⁹ The horns of ungulates grow throughout the animal's life, by the sequential deposition of keratin sheaths over a bony core structure.¹⁹ There is evidence that hormones and the annual cycle of day-length can play important roles in the onset and control of horn growth and cessation, and of growth rate variations with age and seasons.^{21,22}

Capra ibex and *Rupicapra rupicapra rupicapra* are common alpine grazers and we wish to use their horns as isotopic archives and recorders of their behavioural ecology and environment/habitat. *C. ibex* is a highly dimorphic species in which males have longer horns, whereas *R. r. rupicapra* has a discrete sexual dimorphism of horn length.^{23,24} In both species, the horns grow from spring to winter, producing distinct annual increments, i.e. year-rings, whose length decreases asymptotically with age.^{25,26}

Although the horns of ungulates were shown to reflect the isotopic signature of their diet,²⁷ to our knowledge no chronological analyses of horns have been reported, except for one study, which reported the spatial variation of carbon and nitrogen isotopic composition along the growth axis of fossil cattle horn.²⁸ In the present study we determined whether horns contain systematic (spatio-temporal) patterns of isotope composition, and, if so, are the patterns related to ontogenetic changes in animal metabolism (and associated isotope effects) or to inter- and intra-annual variation in the isotopic composition of their diet. We also evaluated if the isotopic composition of contemporaneous horn formation from different regions (sides) of the horn, and contamination of the horn surface with natural compounds (such as suet or other organic materials of plant or animal origin), is a factor that must be considered in horn sample collection and preparation. Minimizing sampling damage to horns is another objective, since horns are often prized trophies and collection items.

Thus, we investigated patterns of horn carbon ($\delta^{13}\text{C}$) and nitrogen ($\delta^{15}\text{N}$) isotopic composition along and perpendicular to the horn axis of *C. ibex* and *R. r. rupicapra*, to answer the following questions: (i) Does the isotope composition of horn sheaths differ between the front and back side of the horn? (ii) Is the surface of the horn substantially contaminated and does this affect the horn isotopic composition? (iii) Does the horn isotope composition change systematically with age, e.g. as a result of ontogenetic changes or chemical/physical weathering, etc? (iv) Do the carbon ($\delta^{13}\text{C}$) and nitrogen ($\delta^{15}\text{N}$) isotope compositions exhibit systematic seasonal (within year-ring) and inter-annual (between year-ring) variation? And finally: (v) Are there any systematic patterns that should be considered in the planning of sampling strategies? Results of this investigation highlight the potential of horns for studies of the ecology of these species and of their habitat, and they provide some practical guidelines for horn sampling, preparation and analysis for different types of research questions.

EXPERIMENTAL

The horns

The study was performed with horns of animals hunted or found dead. Twenty-four horns (one per animal) were sampled: one horn of a *R. r. rupicapra* male from the Ammergau Alps (Germany); and 23 horns of *C. ibex* males, one from Val Trupchun (Swiss National Park, Switzerland) and 22 from Augstmatthorn and Brienzer Rothorn (Natural History Museum of Bern, NHMB, Switzerland).

The *R. r. rupicapra* received no *post mortem* treatment. The horn of the *C. ibex* from Val Trupchun had been boiled in water when the skull was cleaned from adhering tissue and the horn was removed. The horn surface did not receive any other treatment. The horns from the Augstmatthorn and Brienzer Rothorn were collected between 1938 and 2006 and were subject to the routine cleaning and preservation treatments of the museum. These included cleaning and degreasing of the skull and horn, and treatment with insecticide.

Sampling the horns

Horn growth decreases with age for both species, meaning that the year-rings are longer at the tip and become shorter towards the base. Despite the different lengths of the year-rings, each one corresponds to a defined unit of time, produced during a fixed period of the year, between spring and the beginning of winter.²⁹ Therefore, instead of dividing the whole length of the horn into equal sized sections as in hair isotopic studies,¹² each year-ring was sampled separately and divided into equal-length sections (Fig. 1(a)). Although individual sections of year-rings could not be assigned to exact periods of the season (as the exact timing and rate of horn growth were unknown), assessing the spatial variation of isotopic composition within one year-ring was deemed useful to explore (at least qualitatively) seasonal variation of horn isotope composition.

In all instances, samples were collected with a wood-carving knife, which allowed us to remove thin layers of horn (~5 mm long \times 1 mm wide; ~0.2 mg; estimated mean thickness 0.4 mm). On the *R. r. rupicapra* horn, we marked the longitudinal axis of the horn from the tip (oldest part) to the base (youngest part) on both sides of the horn, the front and the back (Fig. 1). We then divided each year-ring into equally dimensioned (~5 mm long) sections. Wide year-rings were divided into a larger number of sections. Thus, eight sections were taken from each of the first three year-rings; five on the fourth; and one each on the fifth, sixth, seventh and eighth ring, yielding 33 sampling positions. This procedure was repeated at each position along the back and front sides of the horn. In addition, at each position and side of the horn, we collected a surface sample and a sub-surface sample just underneath. Thus, in total 132 samples were collected from the *R. r. rupicapra* horn (33 positions \times 2 back/front \times 2 surface/sub-surface).

In *C. ibex*, samples were collected along the longitudinal axis on only the back side of horns. On the individual from Val Trupchun, equally dimensioned sub-surface samples were collected along each year-ring of the horn. Ten samples

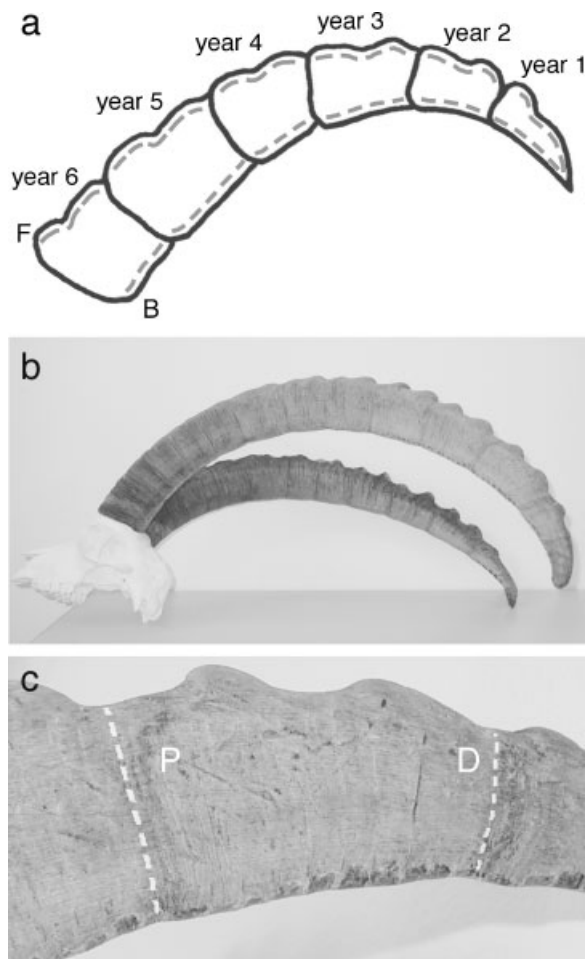


Figure 1. Schematic of sampling a horn of *R. r. rupicapra*. (a) In every year-ring we sampled equal-length sections (grey lines) on opposite positions on the front (F) and back (B) side of the horn. The number of sampling positions varied as a function of year-ring width (see text). For studies of horn contamination we collected (and compared) surface and sub-surface samples at the same positions in one *R. r. rupicapra* and one *C. ibex* horn (see text). (b) The *C. ibex* horn from Val Trupchun and (c) close-up of one year-ring. The white dashed lines give the proximal (P) and distal (D) limit of the year-ring. Horn growth starts in spring, first forming the horn tissue near the distal end of the year-ring. Tissue near the proximal end is formed near the end of the horn growth period, the fall.

were cut on the first eight rings (starting at the tip), five on the 9th, 10th, 11th and 12th, and four on the 13th; the number of samples depending on the length of the year-ring, a total of 104 samples. In addition, to investigate horn surface contamination, surface samples were collected in the third and fourth year-rings, at each sampling position, generating another set of 20 samples.

Sub-surface samples were collected from the other 22 male horns, which originated from the Augstmatthorn and Brienzler Rothorn of Switzerland. Only the beginning of each year-ring, i.e. the distal third of the ring which was formed at the beginning of annual growth in spring, was sampled. This

was done because we were interested in the longer-term (ontogenetic) changes in horn isotope composition and, therefore, wanted to avoid the strong intra-annual isotopic variation in the centre section of the horn. The first year-ring, at the tip of the horn, was often severely eroded and was not sampled. All samples were dried at 60°C for 24 h.

Washing samples

Surface samples from the *C. ibex* horn from Val Trupchun were washed using the protocol described by Schnyder *et al.*¹⁷ for the hair of cows. Briefly, samples were soaked with deionised water and washed in an ultrasonic bath, soaked and centrifuged in methanol/chloroform solution 2:1 (v/v) (at ~60 rpm for 1 h), rinsed with deionised water and dried (48 h, 40°C) before isotope analysis. The presence and isotopic identity of contaminants were assessed by the difference between washed and unwashed samples, and that between unwashed surface samples and corresponding sub-surface samples.

Isotope analysis

Dried samples of ~0.3 to 0.4 mg were enclosed in tin cups and combusted in an elemental analyser (NA 1110; Carlo Erba, Milan, Italy) interfaced (modified ConFlo III; Finnigan MAT, Bremen, Germany) to an isotope-ratio mass spectrometer (Delta Plus; Finnigan MAT). The isotope data, presented as $\delta^{13}\text{C}$ (‰) relative to the PDB standard and $\delta^{15}\text{N}$ (‰) relative to nitrogen in air, were calculated as follows:

$$\delta X = \left[\frac{R_{\text{sample}}}{R_{\text{standard}}} - 1 \right] \times 10^3 \quad (1)$$

where δX is $\delta^{13}\text{C}$ or $\delta^{15}\text{N}$, and R is the respective $^{13}\text{C}/^{12}\text{C}$ or $^{15}\text{N}/^{14}\text{N}$ ratio. The nitrogen and carbon isotope composition of one sample was analysed in the same run using the 'Dual Gas Acquisition' feature of the ISODATNT2.0 software (Finnigan MAT). Laboratory working standard CO_2 and N_2 gases were calibrated against secondary isotope standards (IAEA-CH6 for ^{13}C , accuracy of calibration $\pm 0.13\%$; and IAEA-N1 and -N2 for ^{15}N , accuracy of calibration $\pm 0.15\%$) with the same setup of the system. A solid internal laboratory standard (SILS) with a similar C/N ratio to the horn samples (cattle horn powder $\delta^{13}\text{C}$ -25.63% , $\delta^{15}\text{N}$ 5.68% and C/N ratio 2.91, also calibrated against international standards) was run regularly after every 10th sample as a control. External precision during the investigation (SILS standard deviation) was 0.12‰ for $\delta^{13}\text{C}$ and 0.09‰ for $\delta^{15}\text{N}$; replicated measurements for the same horn sample showed a standard deviation of 0.05‰ for $\delta^{13}\text{C}$ and 0.07‰ for $\delta^{15}\text{N}$.

Carbon isotope discrimination ($^{13}\Delta$)

The horn $\delta^{13}\text{C}$ depends on the carbon isotope composition of atmospheric CO_2 and on fractionation processes associated with the diffusion and fixation of CO_2 during photosynthesis,³⁰ post-photosynthetic fractionations in plants,³¹ and fractionation associated with animal nutritional ecology (e.g. selective grazing) and metabolism.² Since the *C. ibex* horns

from Augstmatthorn-Brienzer Rothorn originated at different times, from 1938 to 2006, their carbon isotopic composition must have been influenced by the long-term isotopic variations of atmospheric CO₂. To remove the effect of atmospheric ¹³C depletion (Suess effect) on horn carbon isotope composition, carbon isotopic discrimination was calculated:

$$^{13}\Delta = \frac{\delta^{13}\text{C}_{\text{CO}_2} - \delta^{13}\text{C}_{\text{horn}}}{1 + \delta^{13}\text{C}_{\text{horn}}/1000} \quad (2)$$

The horn carbon isotope discrimination, ¹³Δ, integrates all fractionation processes associated with the transfer and transformation of CO₂-carbon from the atmosphere, through plants and the animal, into horn carbon.

Carbon isotope composition of atmospheric CO₂

The atmospheric CO₂ carbon isotope composition was obtained from published measurements of CO₂ in free air and in air bubbles separated from ice cores. Free-air data were taken from the following stations: Mauna Loa, Hawaii; Hegyhatsal, Hungary; and Black Sea, Romania; covering the periods 1955–2005³² Data from Antarctica ice cores covered the periods 1938–1978 at Law Dome³³ and 1943–1953 at Siple.³⁴ A double third-order polynomial model was fitted to the atmospheric ^δ¹³C_{CO₂} (‰) data, one for the period 1938–1958 and the other for 1959–2006:

$$\delta^{13}\text{C}_{\text{CO}_2} = m_3t^3 - m_2t^2 + m_1t + m_0 \quad (3)$$

where *t* is time in years; *m*₃ is −2.9E-08, *m*₂ 1.44E-4; *m*₁ −0.240 and *m*₀ 125.57 (*r*² = 0.85) for the period 1938–1958, and 8.4537E-06, −0.051, 101.94 and −72655 (*r*² = 0.97) for the period 1959–2006. The root mean squared error of the combined model for the studied period was 0.09‰.

Statistical analyses

Pairwise comparisons of the mean ^δ¹³C, ^δ¹⁵N and C/N ratio between the groups: front and back samples; surface and sub-surface samples and between washed and unwashed samples, from the same longitudinal sections of the horn, were performed by two-tailed, paired *t*-tests. The differences in ^δ¹³C, ^δ¹⁵N and C/N ratio between front and back sides were investigated in the *R. r. rupicapra* horn (*n* = 34, all year-rings); between surface and sub-surface samples of the *R. r. rupicapra* horn (*n* = 34, all year-rings) and the Val Trupchun *C. ibex* horn (*n* = 21, 3rd, 4th and 5th year-rings); and between washed and unwashed samples for the Val Trupchun *C. ibex* horn (*n* = 21, 3rd, 4th and 5th year-rings).

For presentation of the frequency distribution of the horn keratin C/N ratio, kernel density estimation was performed, because it gives a continuous probability density-function, such that its resolution is not limited by preselected width and end points of bins, as in common histograms. For the theory of kernel density estimation, see Silverman.³⁵ The C/N ratio was estimated for the *C. ibex* horn surface, sub-surface and washed surface samples (each estimation, *n* = 20); and for *R. r. rupicapra* horn surface and sub-surface samples (each estimation *n* = 34).

Multiple regressions, with 'age' and 'year' as independent variables, were used to test for age effects on horn ^δ¹⁵N, ¹³Δ and C/N ratio of *C. ibex*. This was done at the level of the total data set of *C. ibex* from the collection of NHMB, which represented a total time span of 69 years. To isolate the age effects from the small long-term trends of ^δ¹⁵N and ¹³Δ, the data shown in Fig. 3 were corrected for the long-term trend. To further test if the age of the horn year-ring influenced the year-ring isotopic composition, the significance of linear regressions between year-ring age and year-ring ¹³Δ, ^δ¹⁵N and C/N ratio were calculated for all individuals of *C. ibex* (*n* = 23). Significance levels were adjusted to 0.002 following the Bonferroni procedure for multiple testing with an original level of 0.05.

The ^δ¹³C and ^δ¹⁵N patterns along the entire horn and within year-rings were analysed by geostatistical analysis of the horn with most samples per year-ring: the *C. ibex* horn with 10 sections per year-ring, from the 2nd to the 8th year-ring. The variance of δX (which denotes either ^δ¹³C or ^δ¹⁵N) depends on the spatial or temporal separation distance and was quantified by semivariograms (for theory, see³⁶). The empirical semivariogram, $\gamma(h)$, is given as:

$$\gamma(h) = \frac{1}{2N(h)} \times \sum_{i=1}^n [\delta X_i(x_i) - \delta X_{i+h}(x_{i+h})]^2 \quad (4)$$

where γ is the variance for δX between all sample pairs *N* separated by a given number of sections *h*. The distance, *h*, between data points was considered in terms of sections, which correspond to year fractions, as 10 sections were equivalent to 1 year of horn growth. A semivariogram model was then fitted to the empirical semivariogram. The semivariogram model delivers three parameters, the nugget effect, the sill and the range. The nugget effect quantifies the small-scale variance including data uncertainty. The sill quantifies the total variance caused by the nugget effect and the variation due to the spatial pattern. The nugget and sill are also reported as square roots, which deliver the unit ‰ and are equivalent to the standard deviation. The third parameter is the range, which quantifies the number of sections over which the pattern causes autocorrelation. Different types of models can be fitted to the data: our data were fitted best by linear, exponential and periodic models. Linear and exponential models indicate that the maximum variation is not achieved within the data domain, whereas a periodic model indicates a cyclic behaviour of a property.

Two types of semivariograms were calculated for ^δ¹³C and ^δ¹⁵N: the *life-long* semivariogram which included all sample pairs within a distance of up to 50 sections, and the *seasonal* semivariogram which considered only pairs within the domain of a year-ring excluding the variation between years. For the seasonal variation, the seasonal year-ring semivariograms of seven years were pooled to obtain a sufficient *N*.³⁷

Kriging was used to interpolate the ^δ¹³C composition along the horn because it provides the best linear unbiased estimation, which minimises prediction error variances.^{38,39} Kriging was based on the pooled seasonal semivariogram.

Table 1. Differences in horn $\delta^{13}\text{C}$, $\delta^{15}\text{N}$ and C/N ratios of *R. r. rupicapra* and m *C. ibex* between samples of the same transverse section of the horn: front and back side; and between samples from the same point of sampling: surface and sub-surface, and washed surface (surfaceW) and sub-surface. Differences between sample pairs were compared by paired t-test, in *R. r. rupicapra* $n = 68$ and in *C. ibex* $n = 21$; *, $p < 0.05$; n.s., not significant; SD, standard deviation

Layers		Differences (‰)		
		Mean	SD	<i>p</i>
<i>R. r. rupicapra</i>				
$\delta^{13}\text{C}$	front – back	0.00	± 0.21	n.s.
	surface – sub-surface	–0.12	± 0.22	*
$\delta^{15}\text{N}$	front – back	–0.10	± 0.26	*
	surface – sub-surface	0.03	± 0.29	n.s.
C/N	front – back	–0.02	± 0.11	n.s.
	surface – sub-surface	0.11	± 0.11	*
<i>C. ibex</i>				
$\delta^{13}\text{C}$	surface – sub-surface	–0.18	± 0.15	*
	surfaceW – sub-surface	0.06	± 0.16	n.s.
$\delta^{15}\text{N}$	surface – sub-surface	0.07	± 0.23	n.s.
	surfaceW – sub-surface	–0.02	± 0.19	n.s.
C/N	surface – sub-surface	0.13	± 0.06	*
	surfaceW – sub-surface	0.01	± 0.03	n.s.

RESULTS

Isotopic differences between back and front sides and surface and sub-surface of the horn

Paired horn samples from the front and back side of the *R. r. rupicapra* horn, belonging to the same layer (either surface or sub-surface), showed no significant differences in $\delta^{13}\text{C}$ and C/N ratio. A slight, although statistically significant, difference was found between the $\delta^{15}\text{N}$ of the two sides: the back side was about 0.1‰ enriched in ^{15}N relative to the front side (Table 1).

The (unwashed) surface layer differed from the sub-surface layer in $\delta^{13}\text{C}$ and C/N ratio, but no significant difference was observed in $\delta^{15}\text{N}$ (Table 1). The $\delta^{13}\text{C}$ was ~0.1 to 0.2‰ more negative and the C/N ratio was slightly higher in the unwashed surface than in the sub-surface samples. These relationships were virtually the same in both species (Table 1).

The C/N ratio frequency distributions of the horn layers had a similar pattern in both species (Fig. 2): the (unwashed) surface had a wider and non-normal distribution, contrasting with the normal distribution of the sub-surface; and the surface mean value was ~0.1‰ higher than that of the sub-surface. This agreed with the expectation that the unwashed horn surface might contain other substances, with a higher C/N ratio or free of N. The presence of these substances could increase the C/N ratio of surface samples; and – when present in varying proportions – could enlarge and distort the normal distribution curve of the horn C/N ratio. Conversely, the frequency distribution of the C/N ratio of sub-surface samples was normal, as expected for true horn tissue, with mean values similar to those of the horn of the laboratory standard (2.91): 2.95 ± 0.15 and 3.10 ± 0.20 for the *C. ibex* and *R. r. rupicapra*, respectively. After washing the

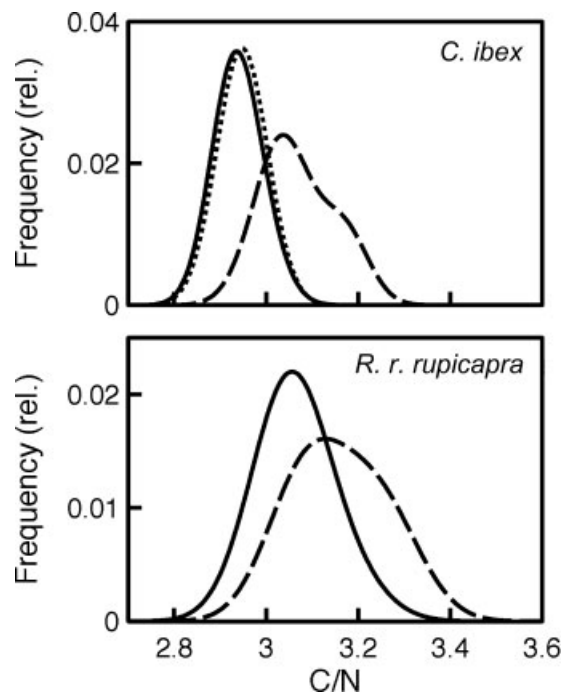


Figure 2. Frequency distributions of carbon-to-nitrogen ratio (C/N) of the surface (dashed lines), sub-surface (solid lines) and washed surface (dotted line) samples of *C. ibex* ($n = 21$) and *R. r. rupicapra* ($n = 32$), calculated from kernel density distribution.

surface samples with organic solvents, the C/N ratios of these samples were virtually the same as that of the sub-surface samples (Fig. 2). Moreover, the pair-wise comparisons of washed surface and sub-surface samples revealed no significant difference in their $\delta^{13}\text{C}$, $\delta^{15}\text{N}$ and C/N ratios ($p > 0.05$) (Table 1).

Amount and isotopic composition of the contaminants on the horn surface

We used a two-member mixing model to estimate the $\delta^{13}\text{C}$ of the contaminant ($\delta^{13}\text{C}_{\text{contaminant}}$) and the contribution of the contaminant ($f_{\text{contaminant}}$) to the carbon content of unwashed surface samples:

$$\delta^{13}\text{C}_{\text{surface}} = f_{\text{contaminant}} \times \delta^{13}\text{C}_{\text{contaminant}} + f_{\text{horn}} \times \delta^{13}\text{C}_{\text{horn}} \quad (5)$$

$$1 = f_{\text{contaminant}} + f_{\text{horn}} \quad (6)$$

with f_{horn} denoting the fraction of horn and $\delta^{13}\text{C}_{\text{horn}}$ the carbon isotope signature of horn. In this estimation, it was assumed that the sub-surface samples were free of contaminants, and so $\delta^{13}\text{C}_{\text{horn}}$ could be equated with $\delta^{13}\text{C}_{\text{sub-surface}}$ ($\delta^{13}\text{C}_{\text{horn}} = \delta^{13}\text{C}_{\text{sub-surface}}$). This was supported by the virtual identity of the $\delta^{13}\text{C}$ of washed surface samples and sub-surface samples (Table 1). In the same way, it was assumed that the C/N ratio of (uncontaminated) horn was the same as that of the sub-surface sample, since the C/N ratios of sub-surface and washed surface samples were the same (Table 1). Lastly, it appeared that the contaminant was free of N (or had a very low N content) as: (i) the C/N ratio of the unwashed surface samples was higher than that of the sub-surface and washed surface samples and (ii) the $\delta^{15}\text{N}$ of sub-surface samples was the same as that of the unwashed

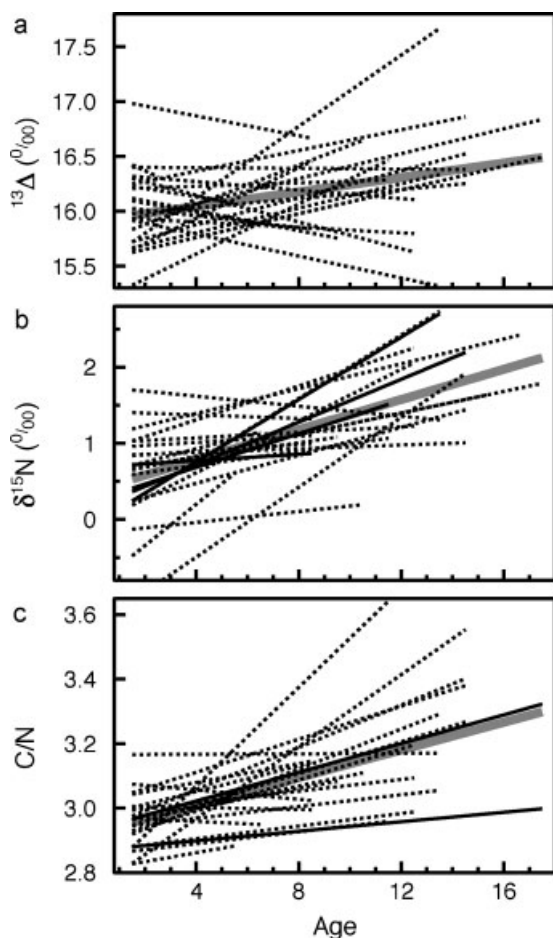


Figure 3. Horn isotopic composition trends with age in *Capra ibex*. Regression lines for all horns ($n=245$, solid thick grey line) and for the horns of individual animals ($n=23$; dotted lines for non-significant relations and solid lines for significant ones, significance level was adjusted following the Bonferroni procedure for multiple testing).

surface samples (Table 1). Thus, f_{horn} was estimated as:

$$f_{\text{horn}} = \frac{C/N_{\text{sub-surface}}}{C/N_{\text{surface}}} \quad (7)$$

Substitution of $\delta^{13}\text{C}_{\text{horn}}$ by $\delta^{13}\text{C}_{\text{sub-surface}}$, combination of Eqn. (7) with Eqn. (5), and rearranging yielded the following equation:

$$\delta^{13}\text{C}_{\text{contaminant}} = \frac{\delta^{13}\text{C}_{\text{surface}} - \left(\frac{C/N_{\text{sub-surface}}}{C/N_{\text{surface}}}\right) \times \delta^{13}\text{C}_{\text{sub-surface}}}{1 - \left(\frac{C/N_{\text{sub-surface}}}{C/N_{\text{surface}}}\right)} \quad (8)$$

which provided estimates of $\delta^{13}\text{C}_{\text{contaminant}}$ from measured variables.

The mean $\delta^{13}\text{C}_{\text{contaminant}}$ of the surface samples was -27.11% ($\pm 0.84\%$ standard error (SE), $n=21$) for the *C. ibex* horn, and -28.82% ($\pm 1.25\%$ S.E., $n=31$) for the *R. r. rupicapra* horn. This meant that the contaminant was depleted in ^{13}C by $\sim 4\%$ relative to the horn in both the *C. ibex* and the *R. r. rupicapra*. However, in both cases, the mean fraction of contaminant ($f_{\text{contaminant}}$) was low (0.04 in

C. ibex and 0.03 in *R. r. rupicapra*), explaining why the contamination had only a small effect ($\sim 0.15\%$) on the $\delta^{13}\text{C}$ of surface samples (Table 1). A similar estimate of the amount of contaminant (4%) in the surface samples was found when comparing the C/N ratios of unwashed and washed surface samples.

Age effects on horn carbon and nitrogen isotope composition

The effects of year-ring age on the carbon isotope discrimination ($^{13}\Delta$), nitrogen isotope composition ($\delta^{15}\text{N}$) and C/N ratio were analysed in all *C. ibex* horns. $^{13}\Delta$ increased slightly with animal age ($+0.03\%$ per year, SE: 0.009) (Fig. 3(a)), but this effect was only evident at the level of the total data set ($p=0.001$). Individual animals exhibited neither consistent (12 animals had positive trends and 11 negative ones) nor significant trends with age. For $\delta^{15}\text{N}$, a stronger trend of 0.1% per year (SE: 0.01) of animal life was observed for the whole group ($p < 0.001$) and positive trends were found for most individuals (21 animals), of which four were statistically significant (Fig. 3(b)). The C/N ratio also increased significantly with age at the whole group level ($+0.021$ per year, SE: 0.003, $p < 0.001$) and positive trends in individuals were frequent (20 animals), although they were statistically significant in just two cases (Fig. 3(c)).

Isotopic patterns along the horns

Within-year-ring (seasonal) and between-year-ring (inter-annual) variation of isotope composition was investigated in one individual each of *R. r. rupicapra* and *C. ibex*. In both individuals the isotopic signatures varied greatly within and between the year-rings (Fig. 4). However, variation of $\delta^{13}\text{C}$ and $\delta^{15}\text{N}$ within year-rings was similar for both animals (mean standard deviation of 0.38%). Significant decreases ($p=0.01$) in $\delta^{13}\text{C}$ and $\delta^{15}\text{N}$ within the 1st year-ring were observed in the *R. r. rupicapra* horn. By contrast the *C. ibex* 1st year-ring revealed an opposite trend of $\delta^{13}\text{C}$ ($p < 0.01$) and a non-significant trend of $\delta^{15}\text{N}$. The latter pattern in *C. ibex* was unexpected as the 1st year-ring is produced in the 1st year of life,²⁹ when weaning occurs and, hence, the horn should be enriched in ^{13}C and ^{15}N .^{40,41} However, wearing or loss of the horn tip may occur, so that the tip of the horn no longer reflects the correct isotopic pattern of the 1st year. In the older year-rings of *C. ibex*, long-term decreasing trends ($p < 0.01$) were observed for both $\delta^{13}\text{C}$ and $\delta^{15}\text{N}$.

In the *R. r. rupicapra* horn the 3rd and 4th year-rings revealed a somewhat similar $\delta^{13}\text{C}$ pattern, less negative at the beginning and end of the ring, and more negative in the centre. However, due to the small dimension of the other year-rings, the number of samples per year-ring was small, and not sufficient to further investigate an underlying seasonal pattern.

Geostatistics was used to analyse the spatial pattern of isotope composition along the *C. ibex* horn. The semivariograms revealed no spatial dependence of the $\delta^{15}\text{N}$ values at the scale of the entire horn (Fig. 5(a)), but substantial dependence at the year-ring scale (Fig. 5(b)), with paired samples differing by up to 0.3% [$(0.07)^{0.5}$] (sill) (Table 2). Conversely, the $\delta^{13}\text{C}$ values exhibited strong spatial dependence at both scales, that of the entire horn (Fig. 5(c)) and that

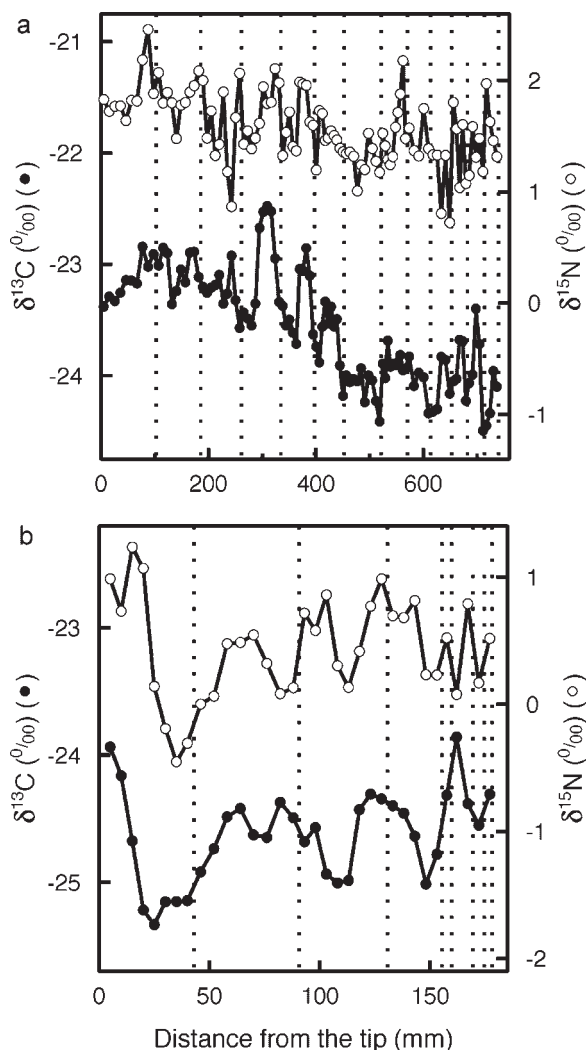


Figure 4. Carbon ($\delta^{13}\text{C}$, ●) and nitrogen ($\delta^{15}\text{N}$, ○) isotope compositions of *C. ibex* (a) and *R. r. rupicapra* (b) horns from the tip to the base using sub-surface samples. Dashed lines refer to the year-rings limits. Note the different scaling of axes for the two species.

of year-rings (Fig. 5(d)). Differences in $\delta^{13}\text{C}$ between neighbouring samples increased linearly with distance at the entire horn, i.e. life-time, scale (Fig. 5(c)), as was expected from the long-term trend of $\delta^{13}\text{C}$ (Fig. 4). The spatial dependence of $\delta^{13}\text{C}$ within year-rings followed a very different periodic pattern (Fig. 5(d)) whose period length (9.6 sections) corresponded almost exactly to the length of the year-ring (10 sections). At this seasonal scale the $\delta^{13}\text{C}$ of sample pairs varied little when they were separated by small or far distances, $\pm 0.16\text{‰}$ [$(0.024)^{0.5}$], but they differed greatly at medium distances (~ 5 sections), $\pm 0.31\text{‰}$ [$(0.09)^{0.5}$]. This pattern was strongly indicative of a systematic seasonal variation of $\delta^{13}\text{C}$.

DISCUSSION

Avoiding sampling artefacts – the roles of sample location and contamination

The surface horn samples were contaminated with carbon compounds, which were depleted in ^{13}C by $\sim 4\text{‰}$ relative to

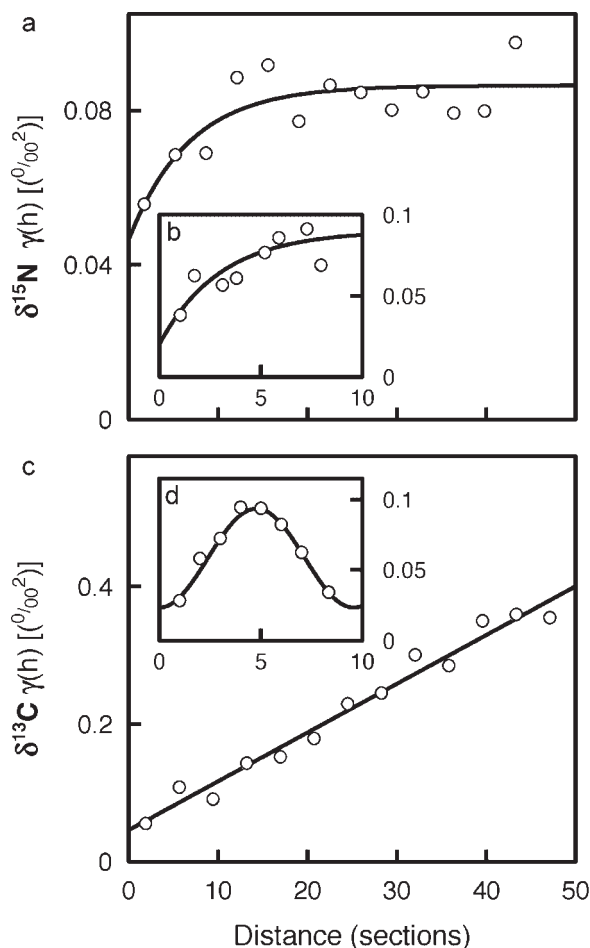


Figure 5. Semivariograms of $\delta^{15}\text{N}$ (a, b) and $\delta^{13}\text{C}$ (c, d) of *C. ibex* horn at the entire-horn (a, c; $h_{\text{max}} = 50$ sections) and year-ring (insets b and d; $h_{\text{max}} = 10$ sections) scales. Semivariograms (a) and (b) were fitted to exponential models $\gamma(h) = \text{nugget} + (\text{sill} - \text{nugget}) \times (1 - \exp(-h/\text{range}))$; (c) to a linear model, $\gamma(h) = \text{nugget} + (\text{sill} - \text{nugget})/\text{range} \times h$; and (d) to a periodic model, $\gamma(h) = \text{nugget} + (\text{sill} - \text{nugget}) \times (1 - \cos(2\pi \times h/\text{range}))$ (see parameters in Table 2). Pooled semivariograms (b) and (d) were calculated from within year-ring data.

the horn material in both *R. r. rupicapra* and *C. ibex*. The contaminant was of an organic nature (as indicated by its $\delta^{13}\text{C}$), appeared to be free of nitrogen and could be removed completely by washing with water and organic solvents. Apparently, it was a natural accretion, since it was found on horns which had not received any protective treatments (such as coating with oleaginous solutions and insecticides, which may be routine treatments in museum collections). The low $\delta^{13}\text{C}$ of the contamination points to fat^{2,31} (e.g. suet) as a major (or sole) component. Since the degree of contamination was small, it had only a relatively small effect ($\sim 0.15\text{‰}$) on the $\delta^{13}\text{C}$ of surface samples in the *R. r. rupicapra* and *C. ibex*. Nevertheless, it is advisable to minimise such contaminants in samples, since the amount may be higher in certain conditions. In some cases we found contaminations of up to 8% of the total sample carbon, and this caused a bias of the $\delta^{13}\text{C}$ of up to 0.4‰ (data not shown). We suggest that there are two equivalent methods to

Table 2. Parameters of the semivariogram models of Fig. 5 for carbon ($\delta^{13}\text{C}$) and nitrogen isotopic composition ($\delta^{15}\text{N}$) along the *C. ibex* horn. *Seasonal* semivariograms include pairs of samples within the same year-rings (maximum distance 9 sections). *Life time* semivariograms considered pairs of samples along the entire horn (maximum distance 50 sections). The *seasonal* semivariograms resulted from pooled year-ring semivariograms. *Nugget* is the semivariance at the origin (distance = 0); *Sill* is the maximum semivariance; *Range* is the maximum distance of spatial correlation, *NSI* is the Nash-Sutcliffe fitting parameter

	Nugget	Sill	Range	Model	NSI
$\delta^{15}\text{N}$					
Seasonal	0.02	0.090	3	Exponential	0.87
Life time	0.047	0.086	6.73	Exponential	0.95
$\delta^{13}\text{C}$					
Seasonal	0.023	0.096	9.56	Periodic	0.98
Life time	0.046	149	21067	Linear	0.99

avoid contamination: (1) washing the surface samples or (2) collection of sub-surface material. Sub-surface samples of both species had normal C/N ratio distributions that were virtually identical to that in the surface layer after washing. Thus, it can be concluded that the sub-surface samples were entirely composed of horn.

The $\delta^{13}\text{C}$ of the horn of *R. r. rupicapra* exhibited significant variation among horn rings along the longitudinal axis (Fig. 4(b)), but $\delta^{13}\text{C}$ of the back and front side of the horn did not differ (Table 1). Thus, although the $\delta^{13}\text{C}$ of horn formation varied strongly over time, the horn material deposited on different sides of each horn ring had the same C isotope composition. The same was true for the C/N ratio of horn. In addition, the $\delta^{15}\text{N}$ was near-identical on the front and back side, except for a small apparent offset of 0.1‰. These results mean that the $\delta^{13}\text{C}$ and $\delta^{15}\text{N}$ patterns along the horn can be reliably reconstructed by sampling a single transect along the horn. This finding is significant as sampling effort can be reduced and damage of the trophy horn minimised by only sampling its back side.

Age effects on horn $\delta^{15}\text{N}$ and carbon isotopic discrimination ($^{13}\Delta$) of *C. ibex*

The $\delta^{15}\text{N}$ and the C/N ratios of year-rings increased significantly with animal age in *C. ibex*. In addition, there was a minimal, but statistically significant effect of age on carbon isotope discrimination. Thus, during the 13 years of an individual's mean life-span, $\delta^{15}\text{N}$ increased by $\sim 1.3\text{‰}$, carbon isotope discrimination by 0.4‰ and C/N ratio by ~ 0.26 . In principle, there are several mechanisms which could produce age-related changes in horn isotope composition, including (i) modifications of horn after its formation as a result of weathering or wear; (ii) changes in diet isotope composition, which could arise from modifications of dietary preferences or altered habitat use/migration patterns with age, or changes in the isotope composition of vegetation over time; and (iii) changes in diet-horn isotope fractionation resulting from altered metabolism or nutritional status. An increase in C/N ratio with age has also been observed in

human finger-nails and this is thought to reflect a change in amino acid composition with age.⁴² Concerning mechanism (i), there is currently no evidence from this or other studies that weathering or wear affects the isotope composition of horn. If it had an effect in the present study, the isotope composition of surface samples should have diverged increasingly from that of sub-surface horn samples along the longitudinal axis of the horn, but this did not happen.

Conversely, changes in diet isotope composition (mechanism (ii)) are a definite possibility in these free-ranging animals. For instance, Grignolio *et al.*⁴³ observed that age had a strong influence on space use by male *C. ibex*. Such behaviour could involve age-dependent shifts between isotopically distinct grazing grounds, but this has not been studied. On the other hand, there were only very minor changes in $\delta^{15}\text{N}$ or ^{13}C discrimination in the sampled *C. ibex* population over the last 70 years (data not shown), proving that the observed age effects on horn isotope composition were true, behaviourally or metabolically based age-effects and were not related to general changes in the isotopic composition of vegetation in the habitat of *C. ibex*.

The effects of animal physiology on the diet-horn isotope fractionation (mechanism (iii)) are also likely to implicate age trends of the isotope composition of *C. ibex* horns. Animal metabolism involves isotopic fractionation: the lighter isotopes are preferentially respired (^{12}C),¹ or absorbed/excreted (^{14}N) during transamination reactions.⁴⁴ Thus, age-related changes in the metabolism of *C. ibex* might lead to metabolic shifts in horn ^{13}C discrimination and $\delta^{15}\text{N}$. Experimental and observational evidence exists that ^{15}N fractionation may depend on growth rate,^{45,46} food restriction,^{45,47,48} age,^{46,48,49} diet nitrogen content,⁵⁰ and quality;^{46,51} although there is not always agreement on the direction and significance of these effects.

In contrast to ^{15}N , variations in ^{13}C isotopic fractionation are mainly attributed to changes in the lipid content of tissues rather than to metabolic traits,⁴⁴ which are not likely to occur in horns as they are essentially composed of protein. Therefore, it is likely that age-related metabolic or nutritional changes explain the increase in horn $\delta^{15}\text{N}$ (and perhaps also $^{13}\Delta$); however, controlled feeding experiments are necessary to determine unambiguously the mechanisms leading to such effects in *C. ibex* horns. Such studies are essential for understanding animal metabolism and related isotope effects, but are challenging because of the relatively long life-span of these animals and the small expected effects: $+0.1\text{‰}$ per year for $\delta^{15}\text{N}$ and $+0.03\text{‰}$ per year for $^{13}\Delta$.

Spatio-temporal patterns of $\delta^{13}\text{C}$ and $\delta^{15}\text{N}$ along the horn

Geostatistical analysis of the spatial distribution of isotope composition of one horn of *C. ibex* indicated two superposed patterns: a multi-annual (life-long) trend of decreasing $\delta^{13}\text{C}$ and seasonal variations of $\delta^{13}\text{C}$. The life-long decrease in $\delta^{13}\text{C}$ was controlled by two mechanisms: the age effect on $^{13}\Delta$ (discussed above) and the decreasing $\delta^{13}\text{C}$ of atmospheric CO_2 . Notably, the contribution of each mechanism was the same: $\delta^{13}\text{C}_{\text{CO}_2}$ decreased by 0.6‰ between 1992 and 2003, and the individuals' age-related $^{13}\Delta$ contributed a further decrease of 0.6‰ in the same period.

While the conversion of positional isotope data into a temporal scale is quite straightforward at the scale of years (since every ring can be assigned to a particular year), this is more difficult at the within-year-ring, intra-annual scale. Indeed, the position-time conversion of within-year-ring information in ungulate horns poses problems similar to those for year rings of trees.⁵² In both cases the seasonal timing and rate of growth must be known. Horns of *C. ibex* grow from spring till winter,²⁹ but more precise information on growth rates is not available. Thus, the chronological record of horn $\delta^{13}\text{C}$ shown in Fig. 6 is necessarily tentative for its exact intra-annual resolution. This record was generated from the positional $\delta^{13}\text{C}$ data (Fig. 4(a)) assuming that horn growth started at the beginning of April, maintained a constant rate, and stopped at the end of November in every year. However, the spatial (Fig. 4(a)) and the temporal (Fig. 6) records prove within-season variations, with large differences occurring during the middle of the growth period (the centre of the year-ring, see Fig. 5(d)) that are either higher or lower than spring or autumn values (Fig. 6). These intra-annual patterns may have resulted from a variety of factors, including (i) seasonal fluctuations in the $\delta^{13}\text{C}$ of atmospheric CO_2 (for instance, the $\delta^{13}\text{C}_{\text{CO}_2}$ amplitude at Hegyhatsal, Hungary is $\sim 0.8\%$ between May and October³²); (ii) seasonal variations of soil and weather conditions which affect plant ^{13}C discrimination, (iii) seasonal migration between isotopically distinct habitats (e.g. movement along altitudinal gradients or between the north and south slopes of the mountain range); or (iv) seasonal variation of within-animal ^{13}C fractionation, possibly triggered by changes in the physiology/nutritional status of the animal related to changes in herbage availability or quality over the seasons. These are all interesting questions which merit further study.

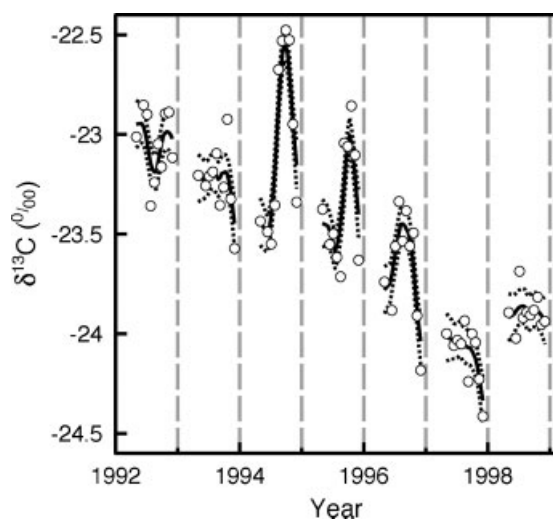


Figure 6. Chronological record of $\delta^{13}\text{C}$ variation in the horn of one individual of *C. ibex*, estimated from positional ^{13}C data (Fig. 4(a)) by assuming a constant horn growth rate from beginning of April to end of November, and a quiescent phase from beginning of December to end of March in all years. The periodic semivariogram model of Fig. 5(d) was used to generate the kriging interpolation line (solid line) and kriging standard deviation (dotted lines).

Whatever the underlying mechanisms, the strong inter-annual differences in the seasonal variation of ^{13}C have practical implications for sampling horns in studies of long-term changes of the ^{13}C signal. Due to the strong seasonal variation among years (mechanisms (i) – (iv) above) the (linear) multi-annual trend constructed from samples collected in the centre part of year-rings was much more ‘noisy’ ($r^2=0.53$) than that obtained from sampling the beginning ($r^2=0.84$) or end ($r^2=0.72$) of the year-rings. Therefore, it is advisable to avoid sampling the centre of year-rings in studies of long-term changes in ^{13}C in the horn of *C. ibex*.

In contrast to $\delta^{13}\text{C}$, the spatial (and temporal) effects on $\delta^{15}\text{N}$ were quite modest and limited to the within-year-ring domain. This indicates that the variation in $\delta^{15}\text{N}$ occurred mainly at the seasonal scale, perhaps due to seasonal migration or alterations of nutritional status. The most evident difference, compared with the spatial pattern of $\delta^{13}\text{C}$, was the continuous change in horn $\delta^{15}\text{N}$ throughout the season in contrast to the cycling pattern of $\delta^{13}\text{C}$.

CONCLUSIONS

This work has established the existence of systematic variations of $\delta^{13}\text{C}$ and $\delta^{15}\text{N}$ in the horn of two common alpine ungulate grazers, which hold valuable information about the nutritional and behavioural ecology of these species. Present evidence indicates some of the variation results from changes in the physiology or nutritional ecology of animals with age, such as the age-effect on $\delta^{15}\text{N}$. Conversely, the multi-annual and seasonal changes of $\delta^{13}\text{C}$ were apparently related to effects of environmental factors on vegetation ^{13}C composition. Further research with GPS-tracked animals and vegetation sampling of grazed areas may help to further resolve effects of behaviour, diet and metabolism on horn isotope composition.

Acknowledgements

The authors would like to thank Max H. O. M. Wittmer for help with geostatistics, Beatrice Blöchliger for assistance in collections from the Natural History Museum Bern, Dr Peter Lüps (formerly at Natural History Museum Bern) for discussions on the *C. ibex* population of the Augstmatthorn and Briener Rothorn, Dr Jürg Paul Müller (Bündner Naturmuseum, Chur) for discussions during the initial stages of this project, Monika Michler for help with sample preparation for isotope analysis, and Professor C. Jerry Nelson (University of Missouri-Columbia) for revising the paper. This work complies with the current laws of Germany and Switzerland, where the work was performed

REFERENCES

1. DeNiro MJ, Epstein S. *Geochim. Cosmochim. Acta* 1978; **42**: 495. DOI: 10.1016/0016-7037(78)90199-0.
2. Tieszen LL, Boutton TW, Tesdahl KG, Slade NA. *Oecologia* 1983; **57**: 32. DOI: 10.1007/BF00379558.
3. Ambrose SH, DeNiro MJ. *Oecologia* 1986; **69**: 395. DOI: 10.1007/BF00377062.
4. Hobson KA. *Oecologia* 1999; **120**: 314. DOI: 10.1007/s004420050865.
5. Kelly JF. *Can. J. Zool.* 2000; **78**: 1.

6. Rubenstein DR, Hobson KA. *Trends Ecol. Evol.* 2004; **19**: 256. DOI: 10.1016/j.tree.2004.03.017.
7. West JB, Bowen GJ, Cerling TE, Ehleringer JR. *Trends Ecol. Evol.* 2006; **21**: 408. DOI: 10.1016/j.tree.2006.04.00.
8. Crawford K, McDonald RA, Bearhop S. *Mammal Rev.* 2008; **38**: 87. DOI: 10.1111/j.1365-2907.2008.00120.x.
9. Tieszen LL, Boutton TW. In *Stable Isotopes in Ecological Research*, Rundel PW, Ehleringer JR, Nagy KA (eds). Ecological Studies, **68**, Springer: New York, 1989; 167–182.
10. Cerling TE, Wittemyer G, Rasmussen HB, Vollrath F, Cerling CE, Robinson TJ, Douglas-Hamilton I. *Proc. Natl. Acad. Sci. USA* 2006; **103**: 371. DOI: 10.1073/pnas.0509606102.
11. Hobson KA, Sease JL. *Mar. Mammal. Sci.* 1998; **14**: 116.
12. Schwertl M, Auerswald K, Schnyder H. *Rapid Commun. Mass Spectrom.* 2003; **17**: 1312. DOI: 10.1002/rcm.1042.
13. West AG, Ayliffe LK, Cerling TE, Robinson TF, Karren B, Dearing MD, Ehleringer JR. *Funct. Ecol.* 2004; **18**: 616. DOI: 10.1111/j.0269-8463.2004.00862.x.
14. Harrison SM, Zazzo A, Bahar B, Monahan FJ, Moloney AP, Scrimgeour CM, Schmidt O. *Rapid Commun. Mass Spectrom.* 2007; **21**: 479. DOI: 10.1002/rcm.2861.
15. Hobson KA, Schell DM. *Can. J. Fish Aquat. Sci.* 1998; **55**: 2601. DOI: 10.1139/cjfas-55-12-2601.
16. Hobson KA, Wassenaar LI, Milá B, Lovette I, Dingle C, Smith TB. *Oecologia* 2003; **136**: 302. DOI: 10.1007/s00442-003-1271-y.
17. Schnyder H, Schwertl M, Auerswald K, Schäufele R. *Global Change Biol.* 2006; **12**: 1315. DOI: 10.1111/j.1365-2486.2006.01169.x.
18. Männel TT, Auerswald K, Schnyder H. *Global Ecol. Biogeogr.* 2007; **16**: 583. DOI: 10.1111/j.1466-8238.2007.00322.x.
19. Marshall RC, Orwin DFG, Gillespie JM. *Electron Microsc. Rev.* 1991; **4**: 47. DOI: 10.1016/0892-0354(91)90016-6.
20. Lubec G, Nauer G, Seifert K, Strouhal E, Porteder H, Szilvassy J, Teschler M. *J. Archaeol. Sci.* 1987; **14**: 113. DOI: 10.1016/0305-4403(87)90001-X.
21. Lincoln GA. *Anim. Reprod. Sci.* 1998; **53**: 87. DOI: 10.1016/S0378-4320(98)00129-8.
22. Toledano-Díaz A, Santiago-Moreno J, Gómez-Brunet A, Pulido-Pastor A, López-Sebastián A. *Anim. Reprod. Sci.* 2007; **102**: 300. DOI: 10.1016/j.anireprosci.2006.10.021.
23. Janis C. *Biol. Rev.* 1982; **57**: 261. DOI: 10.1111/j.1469-185X.1982.tb00370.x.
24. Bro-Jørgensen J. *Evolution* 2007; **61**: 1316. DOI: 10.1111/j.1558-5646.2007.00111.x.
25. Giacometti M, Willing R, Defila C. *J. Mammal.* 2002; **83**: 245. DOI: 10.1043/0022-2372(2002)083(0245:ATISAH)2.0.CO;2.
26. Bassano B, Perrone A, Von Hardenberg A. *Mammalia* 2003; **67**: 65.
27. Cerling TE, Harris JM. *Oecologia* 1999; **120**: 347. DOI: 10.1007/s004420050868.
28. Iacumin P, Bocherens H, Chaix L. *Il Quaternario* 2001; **14**: 41.
29. Ratti P, Habermehl KH. *Z. Jagdwiss.* 1977; **23**: 188.
30. Farquhar GD, Ehleringer JR, Hubick KT. *Annu. Rev. Plant Phys.* 1989; **40**: 503. DOI: 10.1146/annurev.pp.40.060189.002443.
31. Déines P. In *Handbook of Environmental Isotope Geochemistry*, vol. 1 Fritz P, Fontes JC (eds). Elsevier: Amsterdam, Oxford, New York, 1980; 329–393.
32. NOAA ESRL Global Monitoring Division, 2007. Available: <http://www.esrl.noaa.gov/gmd/dv/ftpdata.html>.
33. Francey RJ, Allison CE, Etheridge DM, Trudinger CM, Enting IG, Leuenberger M, Langenfelds RL, Michel E, Steele LP. *Tellus Ser. B* 1999; **51**: 170. DOI: 10.1034/j.1600-0889.1999.t01-1-00005.x.
34. Friedli H, Oeschger H, Siegenthaler U, Stauffer B. *Nature* 1986; **324**: 237. DOI: 10.1038/324237a0.
35. Silverman BW. *Density Estimation for Statistics and Data Analysis*. Chapman and Hall: London, 1986.
36. Rossi RE, Mulla DJ, Journel AG, Franz EH. *Ecol. Monogr.* 1992; **62**: 277.
37. Voltz M, Webster R. *Eur. J. Soil Sci.* 1990; **41**: 473. DOI: 10.1111/j.1365-2389.1990.tb00080.x.
38. Cressie N. *Math. Geol.* 1990; **22**: 239. DOI: 10.1007/BF00889887.
39. Matheron G. *The Theory of Regionalized Variables and Its Applications*. École de Mines de Paris: Fontainebleau, 1971.
40. Williams JS, White CD, Longstaffe FJ. *Am. J. Phys. Anthropol.* 2005; **128**: 781.
41. Newsome SD, Koch PL, Etnier MA, Aurioules-Gambao D. *Mar. Mammal. Sci.* 2006; **22**: 556.
42. Dittmar M, Dindorf W, Banerjee A. *Gerontology* 2008; **54**: 100.
43. Grignolio S, Rossi I, Bassano B, Apollonio M. *J. Mammal.* 2007; **88**: 1488. DOI: 10.1644/06-MAMM-A-351R.1.
44. Macko SA, Estep MLF, Engel MH, Hare PE. *Geochim. Cosmochim. Acta* 1986; **50**: 2143. DOI: 10.1016/0016-7037(86)90068-2.
45. Sears J, Hatch SA, O'Brien DM. *Oecologia* 2009; **159**: 41. DOI: 10.1007/s00442-008-1199-3.
46. Roth JD, Hobson KA. *Can. J. Zool.* 2000; **78**: 848.
47. Chereil Y, Hobson KA, Bailleul FR, Groscolas R. *Ecology* 2005; **86**: 2881. DOI: 10.1890/05-0562.
48. Oelbermann K, Scheu S. *Oecologia* 2002; **130**: 337. DOI: 10.1007/s004420100813.
49. Overman NC, Parrish DL. *Can. J. Fish Aquat. Sci.* 2001; **58**: 1253. DOI: 10.1139/cjfas-58-6-1253.
50. Pearson SF, Levey DJ, Greenberg CH, del Rio CM. *Oecologia* 2003; **135**: 516. DOI: 10.1007/s00442-003-1221-8.
51. Robbins C, Felicetti L, Sponheimer M. *Oecologia* 2005; **144**: 534. DOI: 10.1007/s00442-005-0021-8.
52. Schleser GH, Helle G, Lucke A, Vos H. *Quaternary Sci. Rev.* 1999; **18**: 927.